



This work is licensed under a Creative Commons Attribution License (CC BY 4.0).

Research article

urn:lsid:zoobank.org:pub:9D6AB063-B8AF-4C96-917F-ED2C121E80A3

Elmidae of Sarawak: the genus *Potamophilus* Germar, 1811, with a description of *P. kelabitensis* sp. nov. (Insecta: Coleoptera)

Ján KODADA^{1,*}, David S. BOUKAL², Peter VĎAČNÝ³,
Katarína GOFFOVÁ⁴ & Kamila ONDREJKOVÁ⁵

^{1,3,4,5} Department of Zoology, Faculty of Natural Sciences, Comenius University in Bratislava,
Ilkovičova 6, SK-84215 Bratislava, Slovakia.

² Department of Ecosystem Biology, Faculty of Science, University of South Bohemia &
Department of Biosystematics and Ecology, Biology Centre AS CR, Institute of Entomology,
Branišovská 31, CZ-37005 České Budějovice, Czech Republic.

* Corresponding author: jan.kodada@uniba.sk

² Email: boukal@entu.cas.cz

³ Email: peter.vdacny@uniba.sk

⁴ Email: katarina.goffova@uniba.sk

⁵ Email: kamila.ondrejкова@gmail.com

¹ urn:lsid:zoobank.org:author:6E88BFBB-8769-44EC-8285-29E357CEC064

² urn:lsid:zoobank.org:author:79BE655B-7B20-41B7-886F-D53BB1E0C5DF

³ urn:lsid:zoobank.org:author:47A28E80-E04F-40C4-93A3-F7F685C9533A

⁴ urn:lsid:zoobank.org:author:4AE3FEFE-E697-43CE-844B-25609A9C0DB1

⁵ urn:lsid:zoobank.org:author:4A685E2B-33AE-4360-BC0A-657422FD64E5

⁵ urn:lsid:zoobank.org:author:43D3B9FA-6218-44D5-B423-BC45F579681B

Abstract. *Potamophilus kelabitensis* sp. nov., a new riffle beetle (Coleoptera, Elmidae) discovered in the Kelabit Highlands (northern Sarawak) and Sapulut environment (southern Sabah), is described. Illustrations of the habitus and diagnostic characters of the new species are presented. Differences from the type species *P. acuminatus* (Fabricius, 1792) from the Palaearctic region, based on DNA barcodes and morphological characters, are discussed. Selected morphological characters of all known species of *Potamophilus* from Vietnam, Myanmar, and Papua New Guinea are also compared with the new species. The systematic position of the genus relative to other sympatric genera of the subfamilies Larainae LeConte, 1861 and selected Elminae Curtis, 1830 belonging to three tribes is discussed based on phylogenetic trees inferred from the mitochondrial COI and nuclear ArgK as well as 18S rRNA gene sequences.

Keywords. Riffle beetles, *Potamophilus*, Borneo, integrative taxonomy.

Kodada J., Boukal D.S., Vďačný P., Goffová K. & Ondřejková K. 2022. Elmidae of Sarawak: the genus *Potamophilus* Germar, 1811, with a description of *P. kelabitensis* sp. nov. (Insecta: Coleoptera). *European Journal of Taxonomy* 806: 1–18. <https://doi.org/10.5852/ejt.2022.806.1695>

Introduction

Germar (1811) established the genus *Potamophilus* for the type species *Parnus acuminatus* Fabricius, 1792 from Germany. The type species is widely distributed in the Palaearctic region, where it is reported from 28 countries (Jäch *et al.* 2016). Although widely distributed, the species is usually rarely sampled, often with a small number of adult specimens. Many European records are old, dating back to the first half of the last century, and the species is classified as strongly in danger of extinction (e.g., Boukal 2005; Jäch *et al.* 2005). Adults are active flyers and are often attracted by light traps; they develop in running waters and inhabit larger streams and rivers, mostly preferring hypopotamal regions.

The known habitat characteristics and bionomy of the genus are based on studies of the type species. The larvae of *P. acuminatus* are obligatorily xylophagous and feed on submerged dead wood of deciduous trees in running water, and their development lasts up to several years (e.g., Gerber 1993; Jäch *et al.* 2005; Kodada pers. obs.) while the short-lived adults feed on the leaves of aquatic mosses such as *Fontinalis antipyretica* L. New data show that the species is not as rare as formerly assumed (Buczyński *et al.* 2011; Csabai *et al.* 2010; Kálmán *et al.* 2009). This may reflect the combined effects of a better knowledge of the species bionomy, targeted field surveys, and gradually improving water quality in many larger European rivers in the past decades.

On the other hand, there are no data on the ecology, distribution, and larval development of the other four described species of *Potamophilus*. These include *P. albertisii* Grouvelle, 1896 and *P. papuanus* (Carter, 1930) from Papua New Guinea, *P. spinicollis* Delève, 1968 from Vietnam, and *P. feae* Grouvelle, 1892 from Myanmar. These four species are known only from their original descriptions based on singletons or a small or unknown number of specimens (Carter 1930; Delève 1968; Grouvelle 1892, 1896) except for additional published records of *P. albertisii* (Satô 1973).

While the distribution of the known species suggests a much wider geographical range of the genus, it has not previously been reported from the Sunda Islands. In 2018, we collected 20 adults of *Potamophilus* at light at a rather unusual altitude around 900 m a.s.l. in the Kelabit Highlands (villages of Bario and Ramudu) during a collecting trip to Sarawak. A study of the collections deposited at the Natural History Museum in Vienna (2022) revealed four additional specimens collected in the 1990s in southern Sabah. All these specimens represented an undescribed species, and the fresh material also enabled the use of DNA analysis to support species delimitation and test the phylogenetic position relative to sympatric genera of Larainae LeConte, 1861 (*Potamophilinus* Grouvelle, 1896 and *Dryopomorphus* Hinton, 1936) and selected Elminae Curtis, 1830 belonging to three tribes.

Material and methods

Taxonomic methods

The material examined is deposited in the collection of Forest Department Sarawak, Kuching, Malaysia (CFDS), Naturhistorisches Museum Wien, Austria (NHMW), and the Kodada collection, Comenius University in Bratislava, Slovakia (CKB).

Dry specimens were first relaxed for several hours in water with several drops of concentrated acetic acid. Male genitalia were dissected, cleared in lactic acid for 1–2 days, and temporarily mounted in Berlese fluid on a microscope slide with a single cavity. After examination and drawing, the genitalia were mounted in a drop of DMHF (dimethyl hydantoin-formaldehyde resin) on the same card as the respective specimen. Examination and dissections were performed under a Leica M205C stereo microscope with magnifications up to 160× and diffuse LED lighting. Drawings were hand-made using a drawing device (camera lucida) attached to a Leica DM 1000 microscope and subsequently traced in Adobe Photoshop®. The specimens were photographed under a Zeiss Axio-Zoom V-16 stereo microscope with an attached

Canon 5D Mark IV camera. Each stacked habitus photograph was created by stacking 200 focal planes using the software ZereneStacker (<https://zerenesystems.com/cms/stacker>).

The morphological terminology follows Kodada *et al.* (2016) and Lawrence & Ślipiński (2013).

Measurements were made under a Leica MZ205C stereo microscope with a Leica eyepiece cross micrometre. In total, seven morphometric characters listed in the ‘Abbreviations’ section below were scored on 18 specimens. The range of measured values and ratios is followed by mean, standard deviation, and the number of individuals measured. Specimens used for DNA isolation were also included in the datasets.

Molecular methods

Eleven species from nine genera of the family Elmidae Curtis, 1830, including taxa from the subfamilies Larainae and Elminae, were involved in the phylogenetic analyses. The dataset comprised seven species collected during recent field trips to Sarawak (2018–2019): *Ancyronyx sarawacensis* Jäch, 1994; *Ancyronyx pulcherrimus* Kodada, Jäch & Čiampor, 2014; *Dryopomorphus memei* Čiampor, Čiamporová-Zaťovičová & Kodada, 2012; *Graphelmis mumini* Čiampor, 2001; *Potamophilinus* sp.; *Potamophilus kelabitensis* sp. nov.; and *Grouvellinus leonardodicaprio* Freitag, Pangantihon & Njunjić, 2018. Moreover, type species of the genera *Macronychus* Müller, 1806 [type species: *Macronychus quadrituberculatus* Müller, 1806]; *Potamophilus* Germar, 1811 [type species: *Potamophilus acuminatus* (Fabricius, 1792)]; *Stenelmis* Dufour, 1835 [type species: *Stenelmis canaliculata* (Gyllenhål, 1808)]; and *Elmis* Latreille, 1802 [type species: *Elmis maugetii* Latreille, 1802] were also included in the dataset. All sequences were obtained from our material except for the three latter species, whose sequences were retrieved from the GenBank database (<https://www.ncbi.nlm.nih.gov/genbank/>).

All adults intended for DNA extraction were fixed in 96% ethanol; individual tissue samples contained the abdomen or one leg with the coxa and attached muscle. DNA was isolated with the E.Z.N.A.® Tissue DNA kit (OMEGA Bio-tek Inc., Norcross, GA, USA), following the manufacturer’s protocol. The barcoding fragment of the 5’ end of the mitochondrial gene coding for cytochrome *c* oxidase subunit I (COI) was amplified with the standard primers LCO1490 and HCO2198 (Folmer *et al.* 1994). Individual PCR reactions were conducted in a total volume of 15 µl and included 6.67 µl of GoTaq® Green master mix (Promega, Fitchburg, WI, USA), 0.34 µl of each primer (10 pmol/µl), 50 ng of template DNA, and 4.65 µl nuclease-free water. The PCR thermocycler program used for the amplification of the COI fragment was as follows: initial denaturation at 94°C for 180 s, 40 cycles of 94°C for 40 s, 52°C for 40 s, and 72°C for 60 s, and terminal elongation at 72°C for 10 min.

Partial sequences of two nuclear markers, arginine kinase (ArgK) and the 18S rRNA gene (18S), were also analysed. Primers used for their amplification were as follows: AK183F (5’-GAT TCT GGA GTC GGN ATY TAY GCN CCY GAY GC-3’) and AK939R (5’-GCC NCC YTC RGC YTC RGT GTG YTC-3’) for arginine kinase (Wild & Maddison 2008), and 18S5’ (5’-GAC AAC CTG GTT GAT CCT GCC AGT-3’) and 18Sb5.0 (5’-TAA CCG CAA CAA CTT TAA T-3’) for the 18S RNA gene (Shull *et al.* 2001). PCR reactions were set according to the protocols available on ‘The Beetle DNA Lab’ (https://zsm-entomology.de/wiki/The_Beetle_D_N_A_Lab). The quality of PCR products of COI, ArgK, and 18S was checked by electrophoresis in 1% TBE agarose gel. PCR products were purified with the Exo-CIP™ Rapid PCR Cleanup Kit (New England Biolabs® Inc., Ipswich, MA, USA) according to the manufacturer’s instructions. Purified PCR products were sequenced from both directions by MacroGen Europe B.V. (Amsterdam, Netherlands). Sequences were trimmed and assembled into contigs in Geneious ver. 6.1.8 (<https://www.geneious.com>).

Phylogenetic methods

18S rRNA gene sequences were aligned in MEGA-X (Kumar *et al.* 2018), using the Muscle algorithm. The nucleotide sequences of the two protein-coding genes were aligned with the Muscle codon algorithm, considering the invertebrate mitochondrial genetic code in the case of COI and the standard genetic code in the case of the nuclear ArgK gene. Phylogenetic trees were constructed in maximum likelihood (ML) and Bayesian frameworks. ML analyses were conducted in IQTREE ver. 1.6.10 (Nguyen *et al.* 2015) on the IQ-TREE web server (<http://iqtree.cibiv.univie.ac.at/>) (Trifinopoulos *et al.* 2016). Each molecular marker was assigned the best evolutionary substitution model, as chosen by the in-built program under the Bayesian Information Criterion. The branching pattern was assessed with 1000 ultrafast bootstrap replicates, whereby the ‘bnni’ algorithm was employed to reduce overestimating nodal support (Hoang *et al.* 2018). Bayesian inferences were carried out in MrBayes ver. 3.2.7 (Ronquist *et al.* 2012). Prior parameters of evolutionary models of individual molecular markers were estimated with IQTREE and then implemented with the ‘prset’ command. The K2P+I model was assigned to the 18S rRNA gene, the TIM2e+G4 model to ArgK, and the GTR+F+I+G4 model to COI. Markov Chain Monte Carlo (MCMC) simulations included one million generations, each hundredth tree was sampled, and the burn-in fraction was specified to be at 25%. The convergence of MCMC analyses was checked using the in-built MrBayes diagnostics. ML and Bayesian trees were computed as unrooted and were rooted with the outgroup taxa in FigTree ver. 1.2.3 (<http://tree.bio.ed.ac.uk/software/figtree/>). Finally, pairwise uncorrected *p*-distances of 18S, ArgK, and COI nucleotide sequences of *Potamophilus* spp. and *Potamophilinus* sp. were calculated in MEGA-X (Kumar *et al.* 2018).

Abbreviations

- EL = elytral length measured from the most anterior margin of the elytron to the most posterior point of the elytron in the dorsal aspect
- EW = greatest width of elytra in the dorsal aspect
- HW = head width including eyes
- ID = minimum linear distance between eyes in the dorsal aspect
- PEL = linear distance between the anterior margin of the pronotum and the apex of the elytra along the midline
- PL = pronotal length along the midline
- PW = maximum pronotal width

Results

Phylogenetic analysis

Eight new COI sequences were obtained from three Larinae and five Elminae taxa. In addition, new partial sequences of ArgK and 18S were acquired from three Larinae and five Elminae species. Their origin and GenBank accession numbers are summarised in Table 1.

Maximum likelihood and Bayesian trees inferred from the concatenated 18S, ArgK, and COI dataset (1872 nucleotide positions) had identical topologies. Therefore, posterior probabilities (PP) from Bayesian analyses were mapped along with bootstrap support onto the best scoring ML tree (Fig. 1). *Potamophilus kelabitensis* sp. nov. grouped with *P. acuminatus* with maximum statistical support. Given the present taxon sampling, *Potamophilinus* sp. was depicted as their nearest relative with strong support (82% ML bootstrap, PP = 0.98). *Dryopomorphus memei* clustered with three representatives of the subfamily Elminae (i.e., *Elmis maugetii*, *Grouvellinus leonardodicaprioi*, and *Macronychus quadrituberculatus*) though with very low statistical support (63% ML, PP = 0.94) that questions its phylogenetic position within this clade. The remaining members of the subfamily Elminae formed a homogenous and very

Table 1. Origin and GenBank accession numbers of molecular markers used in phylogenetic analyses (codes after species names refer to voucher specimens used for DNA extraction).

Sample	Locality	GenBank accession no		
		COI	ArgK	18S
Newly obtained sequences				
Larainae				
<i>Dryopomorphus memei</i> JK006	Malaysia, Sarawak, Bario env.	MW649802	MW648992	MW650893
<i>Potamophilinus</i> sp. JK022	Malaysia, Sarawak, Bario env.	MW649803	MW648993	MW650894
<i>Potamophilus kelabitensis</i> JK540	Malaysia, Sarawak, Bario env.	MW649804	MW648994	MW650895
Elminae				
<i>Macronychus quadrituberculatus</i> JK531	Slovakia, Studienka, Rudava riv.	MW649805	MW648995	MW650896
<i>Grouvellinus leonardodicaprio</i> JK044	Malaysia, Sarawak, Bario env.	MW649806	MW648996	MW650897
<i>Graphelmis mumini</i> JK003	Malaysia, Sarawak, Bario env.	MW649807	MW648997	MW650898
<i>Ancyronyx sarawacensis</i> JK009	Malaysia, Sarawak, Bayur riv.	MK505396	MW648998	MW650899
<i>Ancyronyx pulcherrimus</i> JK077	Malaysia, Sarawak, Gunung Mulu	MW649808	MW648999	MW650900
Published sequences				
Larainae				
<i>Potamophilus acuminatus</i>	For origin, see GenBank	HM422045	MF470044	AF451911
Elminae				
<i>Elmis maugetii</i>	For origin, see GenBank	MW684762	MF470036	AF451916
<i>Stenelmis canaliculata</i>	For origin, see GenBank	KU918110	LC426355	AF451919

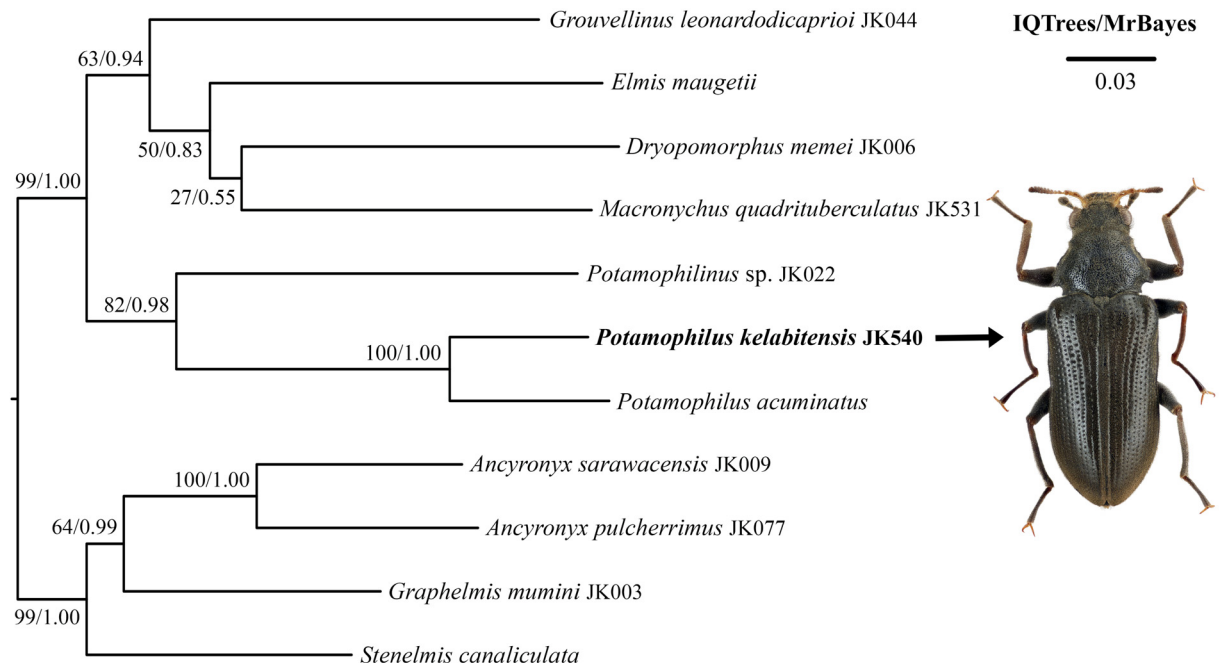


Fig. 1. Phylogenetic tree based on the nuclear 18S rRNA gene (592 nt), ArgK (677 nt), and the mitochondrial COI gene (603 nt). Bootstrap values for maximum likelihood conducted in IQTrees and posterior probabilities for Bayesian inferences conducted in MrBayes were mapped onto the best scoring ML tree. The scale bar denotes three substitutions per one hundred nucleotide positions.

strongly supported cluster (99% ML, PP = 1.00) in which *Ancyronyx sarawacensis* and *A. pulcherrimus* were grouped with maximum statistical support (Fig. 1).

The separation of *P. kelabitensis* sp. nov. from *P. acuminatus* is undoubtedly corroborated by their deep genetic divergence in the barcoding COI gene (14.3%). The distinctness of *P. kelabitensis* sp. nov. is further strengthened by the comparatively high *p*-distances in the much slower-evolving arginine kinase (5.02%) and the highly conservative 18S rRNA gene (0.17%). These values correspond closely to the evolutionary speed of individual molecular markers as estimated in IQTrees under the respective nucleotide substitution models. Thus, COI is the fastest evolving marker (relative evolutionary speed = 2.1384) followed by ArgK (evolutionary speed = 0.8221), and 18S is the most conservative gene (evolutionary speed = 0.0438) in the present dataset. In other words, our analyses imply that COI evolves ca 2.6 times faster than ArgK, which is reflected by the context-specific divergence between *P. kelabitensis* sp. nov. and *P. acuminatus* in both genes (14.3% in COI vs 5.02% in ArgK). On the other hand, ArgK evolves ca 19 times faster than 18S, causing again a context-specific divergence between the two species of *Potamophilus* (5.02% in ArgK vs 0.17% in 18S). Although the 18S divergence may appear comparatively low, other Elmidae species that are distinct morphologically and conspicuously differ by COI gene sequences could still have identical 18S sequences. Therefore, a single nucleotide difference in this highly conserved gene is strongly indicative of different taxa.

Taxonomy

Class Insecta Linnaeus, 1758
Order Coleoptera Linnaeus, 1758
Suborder Polyphaga Emery, 1886
Superfamily Byrrhoidea Latreille, 1804
Family Elmidae Curtis, 1830
Genus *Potamophilus* Germar, 1811

Potamophilus kelabitensis sp. nov.

urn:lsid:zoobank.org:act:D801EBA4-C36A-4569-B495-7792B4B58F9D

Figs 2–5

Type locality

Malaysia, Sarawak, Miri district, Ramudu. Adults were collected at light in the Pa’Kelapang river environment in the Ramudu settlement (Fig. 5).

Diagnosis

Potamophilus kelabitensis sp. nov. is an elongated, parallel-sided, medium-sized (PEL: 5.3–7.3 mm), predominantly black species with reddish-brown antennal segments 1–4, distal portion of femora, trochanters, anterior face of mesofemora, and claws. The pronotum is about $1.5 \times$ as wide as long, gradually expanded posteriad, widest in front of posterior margin, and deeply excised in hind angles. Pronotal sides are moderately arcuate, finely crenate, and explanate, on each side with conspicuous blunt tooth posteriorly; posterior angles are nearly rectangular. Pronotal surface bears dual punctuation. Large punctures are moderately larger than facets, nearly confluent or separated by distances up to $1.5 \times$ a puncture diameter, punctures appear to be denser laterally. Small punctures are intermixed within larger ones and are moderately larger than those on the head. Elytron with ten punctate striae and one accessory basal stria between the sutural and second stria. Strial punctures on the disc are more prominent than those on the pronotum, separated by one puncture diameter, punctures becoming smaller posteriorly; punctures in striae 6–10 are more prominent, appearing subquadrate and more closely arranged. Intervals are flat, finely punctured; sutural interval moderately raised; elytral apices are slightly deflected and not

meeting at the suture, separated by a gap, narrowly rounded and not protruding. The aedeagus is trilobate, symmetrical; parameres in the apical portion are narrowed, flattened, abruptly bent ventrad, and less sclerotised; apices do not reach the apex of the penis.

Differential diagnosis

The new species differs from all other described species of *Potamophilus* by the following combination of external characters:

- a relatively small size (separating it from *P. feae*);
- distinctly crenate lateral margins of the pronotum (separating it from *P. acuminatus*, *P. albertisii*, *P. feae*, *P. papuanus*, and *P. spinicollis*);
- deeply excised hind angles of the pronotum (separating it from *P. albertisii*);
- lack of impression on the pronotal disc in front of the scutellum (separating it from *P. acuminatus* and *P. spinicollis*);
- flat elytral intervals except the sutural one (separating it from *P. acuminatus*, *P. feae*, and *P. spinicollis*);
- coarse strial punctures on the elytra (separating it from *P. albertisii*);
- subquadrate and not rounded strial punctures in intervals 6–10 (separating it from *P. acuminatus*, *P. feae*, *P. papuanus*, and *P. spinicollis*);
- evenly rounded elytral apices in both sexes (separating it from *P. acuminatus*, *P. albertisii*, *P. feae*, and *P. papuanus*);
- the absence of a distinct, well-separated median tubercle on the meso- and metatibia in males (separating it from *P. albertisii*, *P. feae*, *P. papuanus*, and *P. spinicollis*).

For the sake of convenience, brief diagnoses of the described species are given below.

In *P. acuminatus* (PEL: ca 6.1–7.7 mm), the hind angles of the pronotum are deeply excised, pronotal sides are smooth, not crenate; pronotal disc with a wide, distinct depression in front of the scutellum. Strial punctures on the elytra are moderately coarse, sharply impressed, rounded, and separated by about their diameter. Elytra are long and narrow (ca 3.6–4.0 × as long as pronotum), with the first interval raised in the posterior 0.8 of its length, distinctly convex intervals 3 and 5, and other intervals flat to feebly convex. The apex of each elytron is produced, angulate in males while acuminate and more protruding with divergent apices in females. Meso- and metatibia are weakly sinuous; mesotibia in males is usually more strongly enlarged distally with an indistinct median tubercle.

In *P. albertisii* (PEL: ca 6.8–7.1 mm), the hind angles of the pronotum are at most slightly emarginated, with the emargination at most half as wide as scutellum; pronotal sides are smooth, not crenate; pronotal disc is flat or at most indistinctly impressed in front of the scutellum. Strial punctures on the elytra are moderately fine to fine, conspicuously sharply impressed, elongate, and separated by about 1–2 × their length. The first elytral interval is raised, and the remaining intervals are flat or at most slightly convex, similarly as in *P. kelabitensis* sp. nov. The apex of each elytron is produced, angulate in males and acuminate in females, with subparallel apices. Meso- and metatibia are weakly sinuous, usually more strongly so and always with a distinct, acute median tubercle at the distal end of both tibiae in males.

In *P. feae* (PEL: ca 9.5–10.4 mm), the hind angles of the pronotum are deeply excised; pronotal sides are smooth, not crenate; pronotal disc is at most indistinctly impressed in front of the scutellum. Strial punctures on the elytra are moderately coarse, more delicate on the declivity, moderately sharply impressed and rounded, separated by about 1–2 × their diameter; first and third interval in the posterior half are distinctly raised, other intervals at most feebly convex. The apex of each elytron is produced, more or less angulate, the angle acute (ca 60°), with an almost identical shape in both sexes. Mesotibia is weakly

sinuous, and the distal end bears a stout median tubercle in males; metatibia is almost straight in both sexes.

In *P. papuanus* (PEL: ca 5.4–5.9 mm), the hind angles of the pronotum are deeply excised; pronotal sides are smooth, not crenate; pronotal disc is evenly convex to flat in front of the scutellum. Pronotal disc is densely and finely punctate with the punctures smaller than the eye facets, i.e., the punctuation is finer than in *P. kelabitensis* sp. nov. Elytral intervals are more or less flat, and only the first interval is raised in about the posterior half; striae punctures are rounded, moderately large (slightly larger than eye facets), well and sharply impressed, separated by about 1–2 × their diameter. Elytral apices have an acute angle in males and are angulate to acuminate in females. Mesotibia and metatibia are distinctly curved/sinuate with a blunt tubercle on the mesal face of the distal part in males, nearly straight or only weakly sinuate in females.

In *P. spinicollis* (PEL: ca 7.0 mm), the hind angles of the pronotum are deeply excised; pronotal sides are smooth to indistinctly and irregularly crenate, especially in the posterior half; pronotal disc with a distinct subtriangular depression in front of the scutellum. Elytral intervals are convex on the disc, with the first interval raised in the posterior 0.8 of its length. Strial punctures are rounded and conspicuously coarse, larger than those on the pronotum and much larger than eye facets, well and sharply impressed, separated by at most their diameter on the disc, smaller and sparser towards the lateral sides and posterior declivity. Male with the apex of each elytron separately rounded (female unknown) and with a rather prominent, pointed tubercle on the mesal face of the distal part of meso- and metatibia.

Etymology

The species is named after the Kelabit Highlands, an isolated highland plateau in the interior of the Sarawak State (Malaysia) and bordering the Kalimantan Province (Indonesia).

Type material

Holotype

MALAYSIA • ♂; “Malaysia, Sarawak, Miri distr., Ramudu, 26.06.2018, (15) 3°33'17.0" N 115°29'38.5" E 921 m a.s.l., Pa'Kelapang riv. env., J. Kodada & D. Selnekovič lgt., at light”; CFDS.

Paratypes

MALAYSIA • 11 ♂♂, 7 ♀♀; same collection data as for holotype; CFDS, CKB • 1 ♀; “Malaysia, Sarawak, Miri distr., Bario, 19.–23.6.2018, Lian Labang Garden, at light, J. Kodada & D. Selnekovič lgt.”; CKB JK540 • 2 ♂♂, 2 ♀♀; “Malaysia, Sabah, Batu Punggul Resort env., river in primary forest, 25.Vi. 1990”; NHMW.

Measurements (all values in mm)

PEL: ♂♂ 5.31–5.46 (5.39 ± 0.06, n = 11), ♀♀ 5.77–6.93 (6.18 ± 0.36, n = 7); PL: ♂♂ 1.31–1.36 (1.32 ± 0.03, n = 11), ♀♀ 1.46–1.51 (1.51 ± 0.07, n = 7); PW: ♂♂ 1.91–1.97 (1.97 ± 0.09, n = 11), ♀♀ 2.07–2.57 (2.24 ± 0.16, n = 7); EL: ♂♂ 4.09–4.19 (4.14 ± 0.04, n = 11), ♀♀ 4.39–5.30 (4.76 ± 0.28, n = 7); EW: ♂♂ 2.12–2.22 (2.18 ± 0.03, n = 11), ♀♀ 2.42–3.14 (2.61 ± 0.23, n = 7); HW: ♂♂ 1.21–1.26 (1.25 ± 0.03, n = 11), ♀♀ 1.31–1.51 (1.37 ± 0.06, n = 7); ID: ♂♂ 0.71–0.80 (0.76 ± 0.27, n = 11), ♀♀ 0.81–0.91 (0.84 ± 0.05, n = 7).

Description

Holotype

The description of the holotype is completed by figures of the holo- and paratype specimens (Fig. 2).

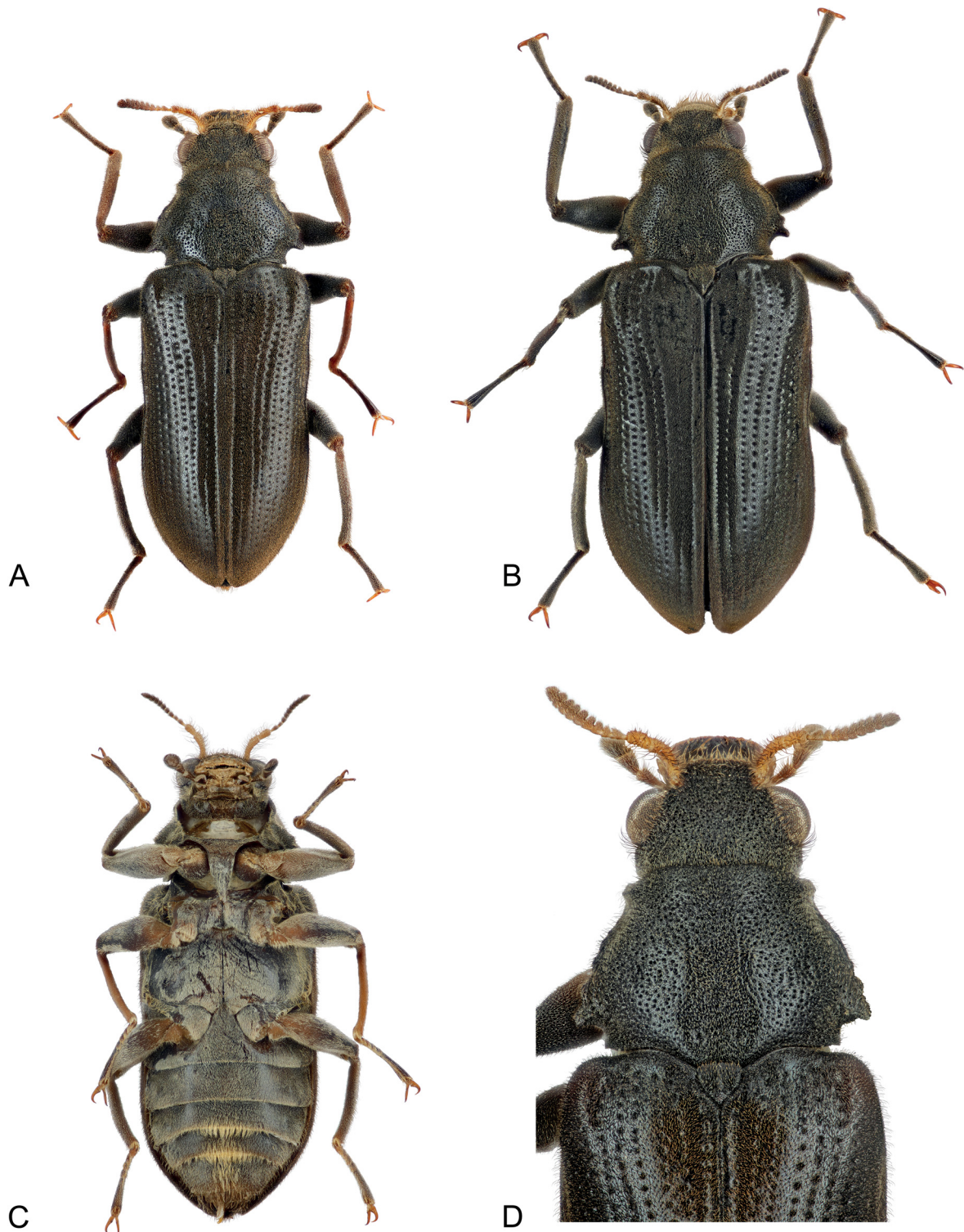


Fig. 2. *Potamophilus kelabitensis* sp. nov. **A.** Male holotype (CFDS), dorsal view, length from anterior margin of clypeus to elytral apex: 5.90 mm. **B.** Female paratype (CKB), dorsal view, length from anterior margin of clypeus to elytral apex: 7.31 mm. **C.** Male paratype (CKB), ventral view. **D.** Detail of the head, pronotum, and anterior portion of elytra, male paratype (CKB).

BODY (Fig. 2A). Elongated, about $2.5 \times$ as long as wide (PEL/EW), parallel-sided, and moderately convex. Length including head 5.90 mm, maximal width across elytra 2.1 mm. Overall colour black; antennal segments 1–4, ventral mouthparts, distal portion of femora, trochanters, anterior face of mesofemora, and claws reddish-brown. Vestiture consists of longer, more or less erect setae and short, strongly recumbent, hair-like setae. Longer setae acute, in narrow sockets; dorsal ones moderately dense, brownish. Ventral setae yellowish, denser on lateral portion of thorax, posterior and lateral portion of ventrites, mainly on ventrites 3–5 and on coxae and trochanters (Fig. 2C). Short setae in narrow sockets (micropunctures), moderately densely to densely arranged, especially ventrally very dense.

HEAD (Fig. 2D). Moderately wider than long, large (HW: 1.2 mm), moderately declined dorsally, arched laterally and flattened ventrally; slightly retracted into prothorax; frontoclypeal suture finely marked. Labrum transverse, lateral angles rounded, anterior margin feebly emarginated in middle; very dense yellowish setae in close rows along anterior margin and laterally; surface finely punctured, with numerous longer setae. Anterior margin of clypeus straight, bordered by a row of longer setae, clypeus moderately shorter than labrum. Frons without sublateral depressions, surface densely punctured, puncture diameter slightly larger than a facet diameter, punctures separated by $0.5\text{--}1.5 \times$ puncture diameter; interstices shiny, with micropunctures. Eyes large and strongly protuberant (ID: 0.7 mm), nearly circular in lateral view, without interfacetal setae, dorsally surrounded by long conspicuous setae. Antennal insertions exposed from above, close to eye margin; subantennal groove vaguely indicated only, shallow and short. Genae without anterolateral process, with numerous longer setae anteriorly. Gula as wide as long, not in the same plane with mentum, with cavity surrounded by dense hair-like setae; gular sutures straight; submentum short, transverse, densely punctured. Cervical sclerites large, wide and strongly sclerotised. Antenna 11-segmented, serrate, reaching slightly behind anterior margin of pronotum. Scape half as long as ID, moderately curved; posterior face flattened, lacking setae. Pedicel $0.5 \times$ as long as scape, both with conspicuously long, hair-like sensilla; combined length of antennomeres 3–11 moderately longer than combined length of previous antennomeres. Antennomeres 6–10 transverse and more tightly aligned than previous antennomeres. Length/width of antennomeres 1–11 (in mm) as follows: 0.36/0.16: 0.18/0.99: 0.12/0.09: 0.06/0.08: 0.08/0.09: 0.81/0.09: 0.06/0.09: 0.06/0.09: 0.06/0.09: 0.06/0.09: 0.08/0.08. Maxillary palpus four-segmented, shorter than ID; terminal palpomere short, apically enlarged and truncate, with large sensory field; palpomeres 2 and 3 subequal in length, widened distally, with numerous moderately long hair-like sensilla. Mentum flat, short and wide, setose, with sides subparallel; palpigers strongly sclerotised, free, and unfused mesally. Labial palpus three-segmented, half as long as maxillary palpus; first segment short; second segment longer, with short and long hair-like sensilla around apical margin; third segment slightly longer than preceding, with apical sensory field similar to that on maxillary palpus. Ligula short and wide, more strongly sclerotised mesally than anterolaterally; anterior angles rounded, produced laterad.

THORAX. Pronotum $1.47 \times$ as broad as long, PW: 1.95 mm, PL: 1.30 mm, gradually expanded posteriad, widest in front of posterior angles and deeply excised in hind angles. Pronotal sides moderately arcuate, finely crenate and explanate, on each side with conspicuous blunt tooth (projection) posteriorly; posterior angles almost rectangular; anterior angles not protruding. Anterior margin straight, sides with collar-like thickening; posterior margin trisinate. Disc moderately convex, with two small prescutellar foveae, strongly deflexed laterad and anteriorly. Surface with dual punctuation; large punctures moderately larger than facets, nearly confluent or separated by distances up to $1.5 \times$ puncture diameter, appear to be denser laterally. Small punctures moderately larger than those on head, intermixed within larger ones. Hypomerion with ventral outline trisinate, deepest emargination at level of procoxae. Width of hypomerion subequal in middle third, moderately narrowed anteriorly and posteriorly; anterior depression for reception of antennal tip small. Prosternum in front of coxae very short, distinctly shorter than prosternal process, transverse and not concealing head in repose. Prosternal process about twice as long as wide, subtriangular, posterior half distinctly narrowed, sides raised; mesal portion with longitudinal

keel. Procoxae transverse, countersunk; procoxal cavities open posteriorly, moderately widely separated; postcoxal projection absent. Mesoventrite moderately shorter than prosternal process, separated by sutures from surrounding sclerites, posterior angles more or less produced posteriad and overlapping metaventrite; mesoventrite divided by fine discrimen; groove for reception of prosternal process deep, present along entire length, posteriorly widened. Mesocoxae large and prominent, subglobular; mesally separated by distance twice as wide as procoxae. Scutellary shield (scutellum) small, subtriangular, as wide as long, sides arcuate. Metaventrite twice as long as mesoventrite; anterior edge of metaventrite not carinate between mesocoxal cavities, anterolateral portion flat; exposed portion of anepisternum 3 moderately wide and long. Metaventral disc convex on sides, with sizeable medial depression extending from anterior third to posterior margin and with small medial depression anteriorly; discrimen fine, present along entire length of metaventrite; metakatepisternal suture subtle, hardly visible; surface finely punctured. Metacoxae large, transverse, oblique, almost reaching elytra, separated from metaventrite by a suture, posteriorly excavate for reception of femora.

Elytra 4.05 mm long (EL) and 2.15 mm wide (EW), subparallel-sided, moderately convex; each elytron with ten punctate striae and one accessory basal stria between sutural and second stria. Strial punctures on disc moderately larger than those on pronotum, separated by ca distance of puncture diameter, punctures becoming smaller posteriorly; punctures in striae 6–10 larger, appearing subquadrate and more closely arranged; intervals flat, finely punctured; sutural interval moderately raised. Humeri rounded and prominent; lateral margin moderately explanate, inflected at level of metacoxae; anterior margin smooth; elytral apices slightly deflected and not meeting at suture, separated by a gap, narrowly rounded and simple. Epipleura strongly inflected at the level of metacoxae, their width subequal along entire length, oblique and received in deep grooves on meso- and metathorax; posteriorly relatively tightly fitted to abdomen. Hind wing large, darkly pigmented, fully developed. Legs nearly as long as elytra; femoral pubescence short; tibial groove shallow, present on ca distal 0.66. Tibiae moderately longer than femora, slightly curved, nearly straight; pro- and metatibiae with dense short pubescence; mesotibia flattened and lacking dense pubescence, extended and slightly bent at apex with a trace of tubercle. Tarsi five-segmented, ca half as long as tibiae (except claws), pro- and metatarsi densely pubescent; claws simple, similar in form and angle of inclination.

ABDOMEN. Five strongly sclerotised ventrites present, all well separated by sutures; first three ventrites connate, remaining two separated by thin membrane, movable; ventrites moderately convex, shallowly depressed along midline; first ventrite not entirely divided by metacoxae, admedian carinae absent; lengths of ventrites 1–5 (in mm): 0.75: 0.50: 0.35: 0.30: 0.45. Intercoxal process wide, subtriangular, acute anteriorly; lateral margins moderately raised; fifth ventrite truncate posteriorly and shallowly emarginate in middle. Surface of ventrites finely punctured and densely setose; third and fourth ventrites bears conspicuous longer, narrowly spaced, flattened setae near posterior margin; numerous flattened setae also on central and apical portion of fifth ventrite. Male sternite VIII symmetrical, deeply emarginate posteriorly and with numerous dense, long setae; anterior median struts short and thin (Fig. 4D). Tergite VIII dark, well sclerotised, narrowly rounded posteriorly, with dual punctuation and setation. Male sternite IX asymmetrical, anterior median strut long; posterior portion well sclerotised, semitubular, surrounding phallobase; posterior edge shallowly emarginated (Fig. 4C).

AEDEAGUS. Trilobate, symmetrical (Fig. 3A–B), ca 1.30 mm long; phallobase including anterior projection ca $0.7 \times$ as long as parameres, nearly tubular, lateral portions sclerotised, ventral and dorsal portions membranous. Parameres individually articulated with phallobase, dorsally fused near base, ventrally free along whole length; parameres narrowed, flattened, abruptly bent and less sclerotised in apical portion (Fig. 3C), apices do not reach the apex of penis. Penis symmetrical, basal portion expanded ventrally nearly in the form of a ‘bell’; dorsal portion flattened with lateral sides explanate in basal 0.6 and further gradually narrowed apicad, thus penis nearly round in cross-section, with apex bent ventrad; ventral sac membranous without fibula, corona present.

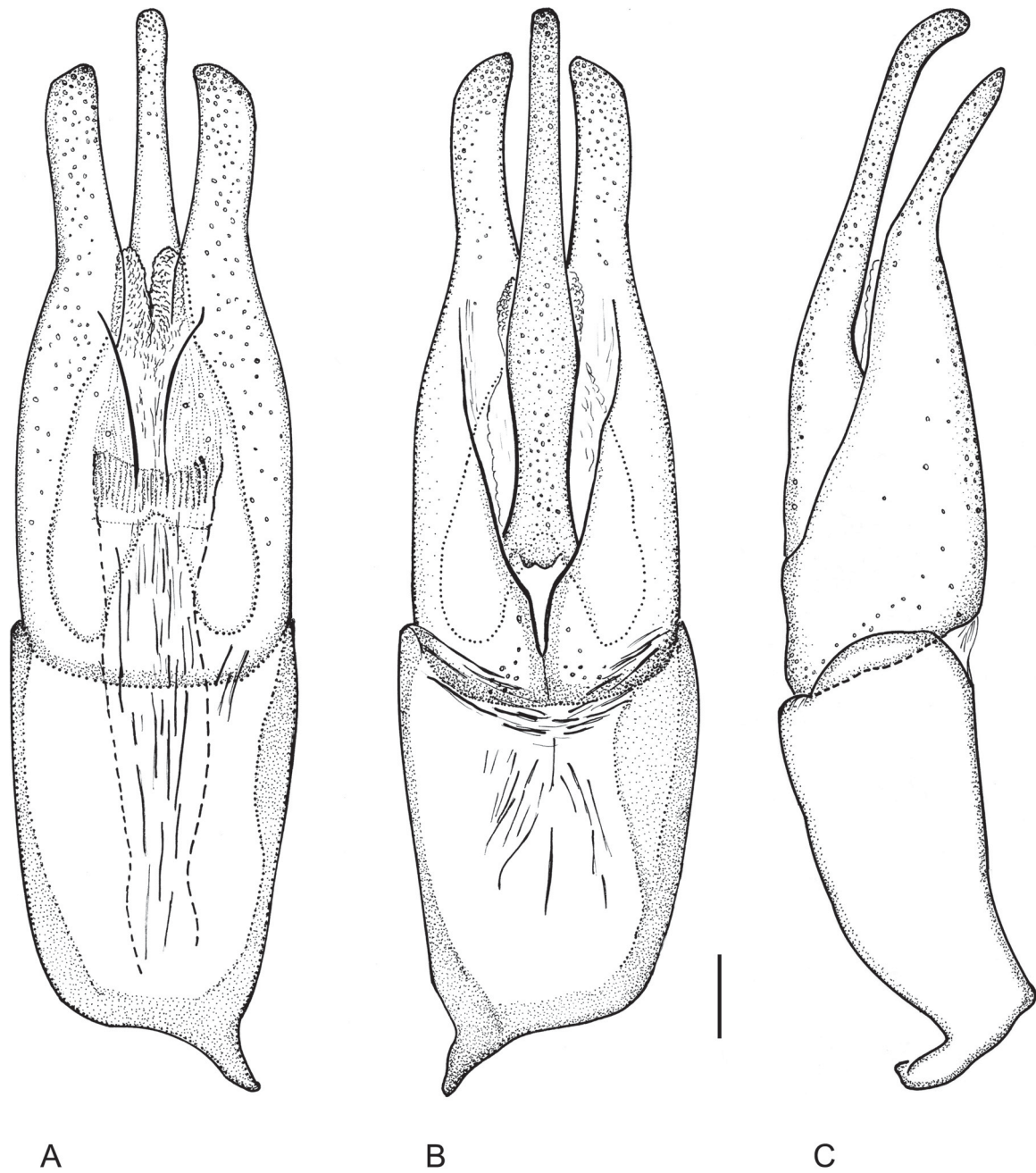


Fig. 3. *Potamophilus kelabitensis* sp. nov., aedeagus of holotype (CFDS). **A.** Ventral aspect. **B.** Dorsal aspect. **C.** Lateral aspect. Scale bar = 0.1 mm.

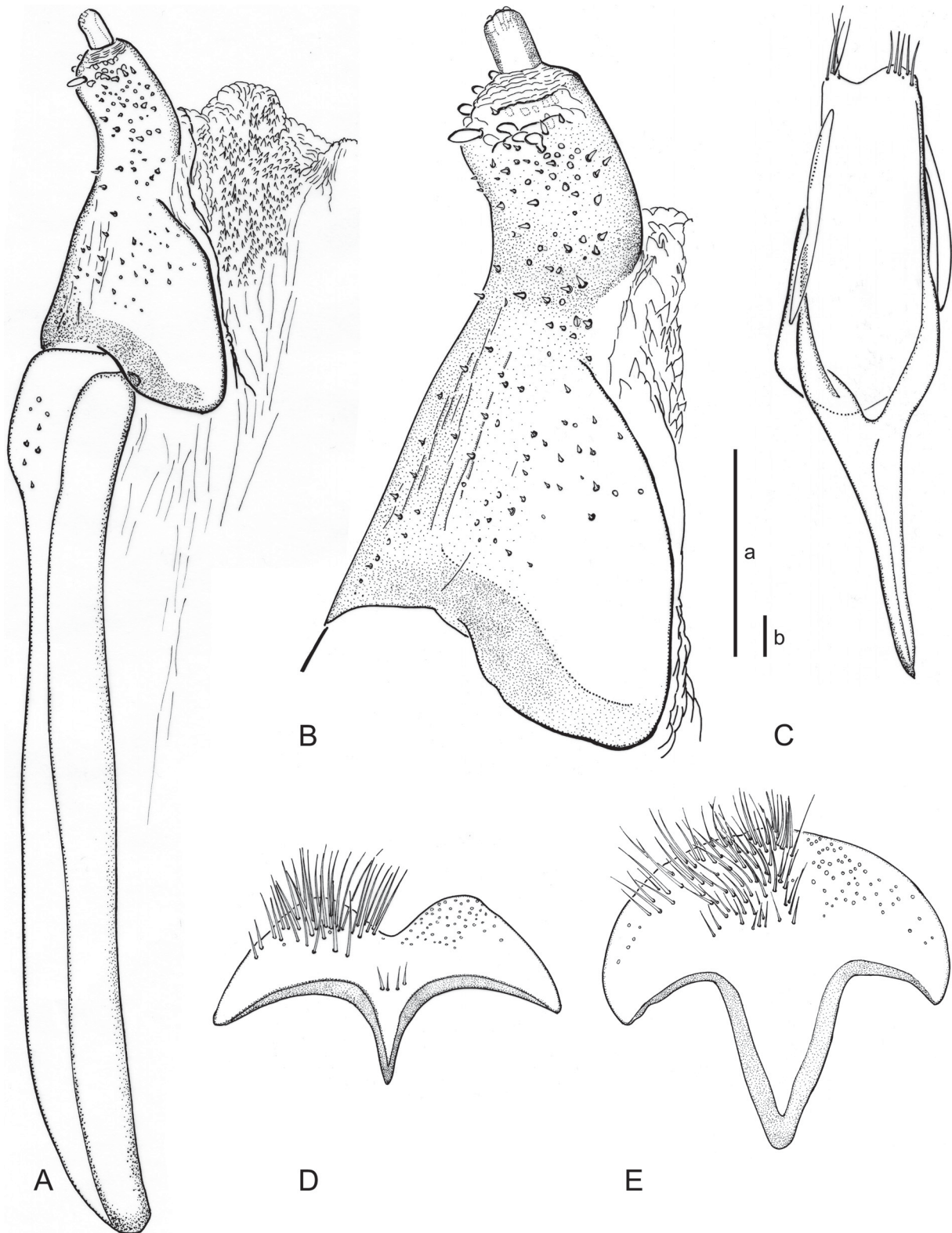


Fig. 4. *Potamophilus kelabitensis* sp. nov. **A.** Ovipositor, ventral aspect. **B.** Distal portion of ovipositor, ventral aspect. **C.** Male segment IX with the spiculum gastrale, ventral aspect. **D.** Male sternite VIII, ventral aspect. **E.** Female sternite VIII, ventral aspect. Scale bars = 0.1 mm; A = a; B–E = b. Specimens: A–B, E = female paratype (CKB); C–D = male holotype (CFDS).

Female terminalia

Posterior margin of female sternite VIII widely rounded; surface with numerous long, dense dark setae (Fig. 4E); anterior margin with robust, subtriangular median strut, the latter subequal in length to posterior portion of sternite. Tergite VIII wider and widely rounded posteriorly; punctuation and setation similar to that of males. Posterior margin of fifth ventrite with a small sharp projection in middle. Ovipositor ca 2.9 mm long, slightly longer than terminal ventrite; valvifers long and robust, ca $2.5\times$ as long as coxite (Fig. 4A); longitudinal baculi wide and well sclerotised. Coxites (preterminal segments) short, widened in dorso-ventral direction; transverse baculi bar-like, distinct, well sclerotised. Coxites not divided by transverse line ventrally (Fig. 4B); distal portion short, narrow and expanded in dorso-ventral direction with a cluster of blunt peg-like sensilla around apex. Stylus very short and bearing small apical sensilla.

Secondary sexual dimorphism

Females (Fig. 2B) are on average longer and broader than males. Their abdominal intercoxal process and the disc of the second and third ventrite are slightly convex, in contrast to the moderately concave (depressed) surfaces in males. In females, the posterior margin of the fifth ventrite is moderately prolonged and pointed in the middle, while in males, it is truncated and shallowly emarginated. The apex of the mesotibia in males is expanded, slightly bent inwards and bears a slight tubercle trace, while it is straight and unexpanded in females.

Variability

Males vary in body length (PEL) from 5.31 to 5.46 mm, females from 5.77 to 6.93 mm. Compared to the holotype, the morphometric characters vary (see measurements above), and there is also minor variation



Fig. 5. The Pa'Kelapang River at Ramudu near the locality where *Potamophilus kelabitensis* sp. nov. was collected.

in the pronotal and elytral punctuation. Pronotal sides are usually moderately arcuate, finely crenate and explanate, on each side with conspicuous blunt tooth posteriorly. The crenate portion varies from finely crenate to deeply crenate between individuals, and the size and form of the posterior teeth also vary from long and subacute, produced posteriad to short and nearly blunt. The teeth on the left and right side of the pronotum are asymmetrical in some specimens.

Distribution

The species is recorded from northern Sarawak and southern Sabah, although the distribution is probably wider across Borneo, given that the type specimens are fully winged and most likely possess excellent flight ability.

Discussion

Habitat association of *P. kelabitensis* sp.nov.

We examined the diversity of Dryopidae Billberg, 1820 and Elmidae in numerous streams in the Kelabit Highlands, Gunung Mulu National Park and the Kuching Division for six months in the years 2018 and 2019. The discovery of a new species, *Potamophilus kelabitensis* sp. nov., was one of the greatest surprises in our research.

As we are well acquainted with the ecology of *P. acuminatus*, we focused on finding larvae and adults of *P. kelabitensis* sp. nov. in their natural habitat. We assumed that the larvae would occur on submerged wood as in *P. acuminatus*, whose large, slow-moving larvae are easy to find in suitable habitats. Moreover, adult *P. acuminatus* can form large clusters of mating individuals on partly submerged wood (Latorica river, Slovakia, Central Europe; Kodada pers. obs.). Surprisingly, our intensive and long-term examination of submerged wood and tree roots in the Ramudu and Bareo environments yielded many adults and larvae of various species of Elmidae (*Ancyronyx* Erichson, 1847, *Leptelmis* Sharp, 1888, and *Graphelmis* Delève, 1968) and Dryopidae (*Stenomystax* Kodada, Jäch & Čiampor, 2003 and *Elmomorphus* Sharp, 1888) but no *Potamophilus* adults or larvae. Neither did we find any places (such as partly submerged wood, or shrubs and trees in the riparian zone) with aggregating adults. We thus cannot fully exclude the possibility that the adults were attracted to the light from a greater distance.

Phylogenetic relationships of *P. kelabitensis* sp. nov. and implications for the classification of Elmidae

Elmidae represent a moderately large beetle family with about 1500 species classified in more than 150 genera that are currently divided in two subfamilies, Larainae and Elminae. The former subfamily contains two tribes, Laraini LeConte, 1861 and Potamophilini Mulsant & Rey, 1872, while the latter subfamily comprises three tribes, Ancyronychini Ganglbauer, 1904, Elmini Curtis, 1830, and Macronychini Gistel, 1848. This framework is rather formal, based on morphological characters, and does not reflect the genuine phylogenetic relationships among elmid genera (e.g., Čiampor & Ribera 2006; Hayashi *et al.* 2019; Jäch *et al.* 2016; Kodada *et al.* 2016). Moreover, the intrafamilial relationships are still largely unknown. The most complex attempt to clarify the phylogenetic relationships of the family so far was based on partial sequences of one mitochondrial and two nuclear genes of 58 Japanese species belonging to 17 genera (Hayashi *et al.* 2019). Three well-supported groups were recognized, although their relationships remained unclear (Hayashi *et al.* 2019). Interestingly, this study suggested a possible synonymy of the genera *Leptelmis*, *Stenelmis*, *Nomuraelmis* Satô, 1963, and *Ordobrevia* Sanderson, 1953 from the Elmini and of the genera *Zaitzevia* Champion, 1923, *Urumaelmis* Satô, 1963, and *Paramacronychus* Nomura, 1958 from the Macronychini. The genus *Dryopomorphus* (formally classified in the Larainae) clustered within the Elminae and was not recognized as a separate lineage.

In the present phylogenetic analyses based on 18S, ArgK, and COI sequences, *Potamophilus kelabitensis* sp. nov. grouped with *P. acuminatus* with maximum statistical support. Given the present taxon sampling, *Potamophilinus* sp. was placed as their nearest relative with medium to strong support. *Dryopomorphus memei* clustered with three representatives of the subfamily Elminae (i.e., *Elmis maugetii*, *Grouvellinus leonardodicaprioi*, and *Macronychus quadrituberculatus*), though with very low statistical support. This questions the phylogenetic position of *Dryopomorphus* in that clade. The remaining members of the subfamily Elminae formed a homogenous and very strongly supported cluster. Nevertheless, the existing formal subfamilial and tribal classifications were not confirmed by our molecular data and are in a need of revision. Therefore, we agree with Hayashi *et al.* (2019) that additional taxon sampling is necessary to elucidate the phylogeny of the Elmidae. Unfortunately, it has become increasingly difficult to obtain permits to collect and export fresh material due to the legislative complexity in many countries.

Acknowledgement

We wish to thank Engkamat Anak Lading and Nur Afiza Bt. Umar (Forest Department Sarawak, Kuching, Sarawak) for the help in arranging the research Permission to conduct research (Permit No. (93) JHS/NCCD/600-7/2/107, Park Permit No. WL49/2018) as well as for help in other administrative processes. Lian Lugun (Forest Department Sarawak, Bario, Sarawak), Suhaily Garauk Riboh (Kampung Ramudu, Sarawak) and Lian Labang Jr. (Bario, Sarawak) accompanied J. Kodada and D. Selnekovič in the Kelabit Highlands near Kampung Ramudu and Bario; their help and field knowledge were irreplaceable. We are very grateful to Janka Poláková (Comenius University, Bratislava, Slovakia) for help with DNA isolation and amplification. We thank two anonymous reviewers, section editor Maxwell Barclay (Natural History Museum, London, United Kingdom), and desk editor Radka Rosenbaumová (National Museum, Prague, Czech Republic) for their comments on the manuscript. The Slovak Research and Development Agency (project APVV-19-0076) and VEGA (project 1/0515/19) partly supported the study.

References

- Boukal D.S. 2005. Elmidae. In: Farkač J., Král D. & Škorpík M. (eds) *Červený seznam ohrožených druhů České republiky. Bezobratlí – Red List of Threatened Species in the Czech Republic*: 462–463. Agentura ochrany přírody a krajiny ČR, Praha.
- Buczyński P., Przewoźny M., Zawal A. & Zgierska M. 2011. On the occurrence of *Potamophilus acuminatus* (Fabricius, 1772) (Coleoptera: Elmidae) in Poland. *Baltic Journal of Coleopterology* 11 (1): 45–56.
- Carter H.J. 1930. Australian Coleoptera. Notes and new species VII. *Proceedings of the Linnean Society of New South Wales* 55 (2): 179–190.
- Csabai Z., Kálmán Z., Kálmán A. & Kovács T. 2010. Further contribution to the aquatic beetle fauna of North-West Hungary (Coleoptera: Hydraedephaga, Hydrophiloidea, Elmidae). *Acta biologica Debrecina. Supplementum oecologica Hungarica* 21: 41–52.
- Čiampor F. & Ribera I. 2006. *Hedyselmis opis*: Description of the larva and its phylogenetic relation to *Graphelmis* (Coleoptera: Elmidae: Elminae). *European Journal of Entomology* 103: 627–636. <https://doi.org/10.14411/eje.2006.084>
- Delève J. 1968. Dryopidae et Elminthidae (Coleoptera) du Vietnam. *Annales historico-naturales Musei nationalis hungarici, Pars Zoologica* 60: 149–181.
- Folmer O., Black M., Hoeh W., Lutz R. & Vrijenhoek R. 1994. DNA primers for amplification of mitochondrial cytochrome *c* oxidase subunit I from diverse metazoan invertebrates. *Molecular Marine Biology and Biotechnology* 3 (5): 294–299.

- Gerber J. 1993. Über den Wiederfund des verschollenen Wasserkäfers *Potamophilus acuminatus* (Fabricius) (Coleoptera: Elmidae) und Beobachtungen zu seiner Bionomie. *Lauterbonia* 13: 89–99.
- Germar E.F. 1811. Eine neue Käfergattung *Potamophilus*. *Neue Schriften der naturforschenden Gesellschaft zu Halle* 1 (6): 41–46.
- Grouvelle A. 1892. Viaggio di Leonardo Fea in Birmania e regioni vicine. L. Nitidulides, Cucujides et Parnides. 2.me Partie. *Annali del Museo Civico di Storia Naturale di Genova* (Serie 2), 12 (XXXII): 833–868.
- Grouvelle A. 1896. Potamophilides, Dryopides, Helmides et Heterocerides des Indes orientales. *Annali del Museo Civico di Storia Naturale di Genova* (Serie 2), 17 (XXXVII): 32–56.
- Hayashi M., Yoshitomi H., Kamite Y., Kobayashi T. & Sota T. 2019. Description of adults and larvae of *Orientalmis parvula* (Nomura & Baba, 1961) (Coleoptera: Elmidae) with their phylogenetic analysis. *Zootaxa* 4568 (3): 483–500. <https://doi.org/10.11646/zootaxa.4568.3.4>
- Hoang D.T., Chernomor O., von Haeseler A., Minh B.Q. & Vinh L.S. 2018. UFBoot2: improving the ultrafast bootstrap approximation. *Molecular Biology and Evolution* 35 (2): 518–522. <https://doi.org/10.1093/molbev/msx281>
- Jäch M.A., Dietrich F. & Raunig B. 2005. Rote Liste der Zwergwasserkäfer (Hydraenidae) und Krallenkäfer (Elmidae) Österreichs (Insecta: Coleoptera). In: Zulka K.P. (ed.) *Rote Listen gefährdeter Tiere Österreichs. Checklisten, Gefährdungsanalyse, Handlungsbedarf. Part 1: Säugetiere, Vögel, Heuschrecken, Wasserkäfer, Netzflügler, Schnabelfliegen, Tagfalter (Grüne Reihe des Lebensministeriums, Vol. 14/1)*: 211–284. Bundesministerium für Land- und Forstwirtschaft, Umwelt und Wirtschaft, Wien.
- Jäch M.A., Kodada J., Brojer M., Shepard W.D. & Čiampor F. Jr. 2016. Coleoptera: Elmidae and Protelmidae. *World Catalogue of Insects, Vol. 14*. Brill, Leiden. <https://doi.org/10.1163/9789004291775>
- Kálmán Z., Kálmán A. & Csabai Z. 2009. Contribution to the Riffle Beetle fauna of Hungary (Coleoptera: Elmidae). *Acta biologica Debrecina, Supplementum oecologica Hungarica* 20: 127–144.
- Kodada J., Jäch M.A. & Čiampor F. Jr. 2016. Elmidae Curtis, 1830. In: Beutel R.G. & Leschen R.A.B. (eds) *Coleoptera, Beetles. Vol. 1: Morphology and Systematics (Archostemata, Adephaga, Myxophaga, Polyphaga partim), Handbook of Zoology, Arthropoda: Insecta (2nd Edition)*: 561–589. Walter de Gruyter, Berlin.
- Kumar S., Stecher G., Li M., Knyaz C. & Tamura K. 2018. MEGA X: Molecular Evolutionary Genetics Analysis across computing platforms. *Molecular Biology and Evolution* 35: 1547–1549. <https://doi.org/10.1093/molbev/msy096>
- Lawrence J.F. & Ślipiński A. 2013. *Australian Beetles. Vol. 1: Morphology, Classification and Keys*. CSIRO, Collingwood. <https://doi.org/10.1071/9780643097292>
- Nguyen L.-T., Schmidt H.A., Haeseler A. von & Minh B.Q. 2015. IQ-TREE: a fast and effective stochastic algorithm for estimating maximum-likelihood phylogenies. *Molecular Biology and Evolution* 32 (1): 268–274. <https://doi.org/10.1093/molbev/msu300>
- Ronquist F., Teslenko M., van der Mark P., Ayres D.L., Darling A., Höhna S., Larget B., Liu L., Suchard M.A. & Huelsenbeck J.P. 2012. MrBayes 3.2: efficient Bayesian phylogenetic inference and model choice across a large model space. *Systematic Biology* 61 (3): 539–542. <https://doi.org/10.1093/sysbio/sys029>
- Satô M. 1973. Notes on dryopoid beetles from New Guinea. *Pacific Insects* 15 (3–4): 463–471.

Shull V.L., Vogler A.P., Baker M.D., Maddison D.R. & Hammond P.M. 2001. Sequence alignment of 18S ribosomal RNA and the basal relationships of Adephagan beetles: evidence for monophyly of aquatic families and the placement of Trachypachidae. *Systematic Biology* 50: 945–969.

<https://doi.org/10.1080/106351501753462894>

Trifinopoulos J., Nguyen L.-T., von Haeseler A. & Minh B.Q. 2016. W-IQ-TREE: a fast online phylogenetic tool for maximum likelihood analysis. *Nucleic Acids Research* 44 (W1): W232–W235.

<https://doi.org/10.1093/nar/gkw256>

Wild A.L. & Maddison D.R. 2008. Evaluating nuclear protein-coding genes for phylogenetic utility in beetles. *Molecular Phylogenetics and Evolution* 48: 877–891.

<https://doi.org/10.1016/j.ympev.2008.05.023>

Manuscript received: 14 May 2021

Manuscript accepted: 23 December 2021

Published on: 17 March 2022

Topic editor: Nesrine Akkari

Section editor: Max Barclay

Desk editor: Radka Rosenbaumová

Printed versions of all papers are also deposited in the libraries of the institutes that are members of the *EJT* consortium: Muséum national d’histoire naturelle, Paris, France; Meise Botanic Garden, Belgium; Royal Museum for Central Africa, Tervuren, Belgium; Royal Belgian Institute of Natural Sciences, Brussels, Belgium; Natural History Museum of Denmark, Copenhagen, Denmark; Naturalis Biodiversity Center, Leiden, the Netherlands; Museo Nacional de Ciencias Naturales-CSIC, Madrid, Spain; Real Jardín Botánico de Madrid CSIC, Spain; Zoological Research Museum Alexander Koenig, Bonn, Germany; National Museum, Prague, Czech Republic.